Int. J. Heat Mass Transfer. Vol. 31, No. 7, pp. 1357–1364, 1988
Printed in Great Britain

0017-9310/88 $3.00 + 0.00
Pergamon Press plc

Natural convection near a rectangular corner

MAN HOE KIM
Department of Mechanical Engineering, Korea Advanced Institute of Science and Technology, P.O. Box 150, Cheongryang, Seoul, Korea

and

MOON-UHN KIM
Department of Applied Mathematics, Korea Advanced Institute of Science and Technology, P.O. Box 150, Cheongryang, Seoul, Korea

(*Received* 7 *September* 1987)

Abstract—The laminar natural convective heat transfer near a rectangular corner formed by the intersection of two vertical quarter-infinite flat plates is considered. For large Grashof numbers, the 'boundary-layer' equations in the corner layer are derived and appropriate boundary conditions are determined using the method of matched asymptotic expansions. Solutions of the equations are numerically obtained for velocity and temperature distributions for Prandtl numbers of 0.72 and 7.0. The cross-flow pattern is quite different from the high-Reynolds number flow along the corner; the simple inflow toward the corner appears, and the swirling motion in the corner is not found.

1. INTRODUCTION

TWO-DIMENSIONAL laminar natural convection boundary-layer flows have been extensively investigated both analytically and experimentally under various surface temperature conditions [1–5]. Many applications in practice require the knowledge of natural convection flow near the surfaces which are composed of simple bodies such as flat plates and cylinders. Of particular interest is the fact that the heat transfer characteristics can be significantly affected by the mutual interaction of the boundary layers. Thus, two-dimensional free convection boundary-layer interactions have received considerable attention in the past.

Merkin and Smith [6] analysed a natural convection boundary layer near two-dimensional corners and sharp trailing edges. Eichhorn and Hasan [7] calculated the mixed convection for flow over a wedge. Hartfield and Edwards [8] studied the effect of adiabatic wall extensions attached at the end of the downward facing heated horizontal plate. On the other hand, three-dimensional boundary-layer interactions have received little attention. Liu and Guerra [9] studied theoretically the natural convection flow in a saturated porous medium near a concave corner formed by two vertical quarter-infinite flat plates. They calculated temperature profiles and Nusselt number for a corner of various angles and discussed the interaction between the two plates.

The present study analyses the natural convection heat transfer along a vertical rectangular corner. The corner layer equations which govern the behaviour of laminar natural convection flow near the corner are derived and appropriate boundary conditions are determined using the method of matched asymptotic expansions similar to the scheme used by Rubin [10] for the incompressible high-Reynolds number flow along a rectangular corner. Numerical results by the finite difference method are presented for fluids with a Prandtl number of 0.72 (such as air) and 7.0 (such as water).

2. ANALYSIS

Consider the laminar natural convection flow along a rectangular corner depicted in Fig. 1. The flow is partitioned into the three regions (Fig. 1(b)), since the characteristics of the flow in the respective regions are different; Region I away from two plates is denoted as the potential flow, Regions II and III near the plates as the boundary layers, and Region IV near the corner as the corner layer. Region IV is a region of overlap of two boundary layers where the inflow of one plane becomes the secondary flow of the other. Solutions for the boundary layers and potential flow are obtained by the method of matched asymptotic expansions and the results are used as the asymptotic boundary conditions for the corner layer.

2.1. *Corner layer equations*

Using the Boussinesq approximation and neglecting the viscous dissipation in the fluid, the governing equations are given by

$$\frac{\partial u^*}{\partial x} + \frac{\partial v^*}{\partial y} + \frac{\partial w^*}{\partial z} = 0 \tag{1a}$$

$$\frac{\mathrm{D}u^*}{\mathrm{D}t} = -\frac{1}{\rho}\frac{\partial p^*}{\partial x} + \nu\nabla^{*2}u^* + g\beta(T - T_\infty) \tag{1b}$$

NOMENCLATURE

a grid spacing parameter
Gr local Grashof number, $g\beta\Delta Tx^3/\nu^2$
h local heat transfer coefficient
k thermal conductivity
N, S transformed independent variables
Nu local Nusselt number
p^* pressure in x, y, z coordinate system
p pressure in ξ, η, ζ coordinate system
Pr Prandtl number, ν/α
q local surface heat transfer rate per unit area
r magnitude of cross-flow velocity
T temperature
T_w wall temperature
T_∞ ambient temperature
ΔT temperature difference, $T_w - T_\infty$
u^*, v^*, w^* velocity components in x, y, z directions
u, v, w velocity components in ξ, η, ζ directions
$\bar{u}, \bar{v}, \bar{w}$ velocity components in boundary layer
U, V, W velocity components in the potential flow
U_c convective velocity, $\frac{1}{2}(g\beta\Delta Tx)^{1/2}$
x, y, z Cartesian coordinate defined in Fig. 1
$\bar{x}, \bar{y}, \bar{z}$ dimensionless variables.

Greek symbols
α thermal diffusivity
β thermal expansion coefficient
γ $\lim_{\eta\to\infty}[\eta f'(\eta) - 3f(\eta)]$
θ dimensionless temperature
Θ direction of cross-flow velocity
μ dynamic viscosity
ν kinematic viscosity
ξ, η, ζ scaled independent variables (Fig. 1)
ρ density of fluid
τ_w wall shear stress
$\tau_{w\infty}$ wall shear stress as $\zeta \to \infty$, $\eta/\zeta \to 0$
ϕ, ψ velocity potential defined in equations (16)
Φ velocity potential for potential flow
Ω streamwise vorticity function defined in equations (17).

$$\frac{Dv^*}{Dt} = -\frac{1}{\rho}\frac{\partial p^*}{\partial y} + \nu\nabla^{*2}v^* \tag{1c}$$

$$\frac{Dw^*}{Dt} = -\frac{1}{\rho}\frac{\partial p^*}{\partial z} + \nu\nabla^{*2}w^* \tag{1d}$$

$$\frac{DT}{Dt} = \alpha\nabla^{*2}T \tag{1e}$$

where

$$\frac{D}{Dt} \equiv u^*\frac{\partial}{\partial x} + v^*\frac{\partial}{\partial y} + w^*\frac{\partial}{\partial z}$$

$$\nabla^{*2} \equiv \frac{\partial^2}{\partial x^2} + \frac{\partial^2}{\partial y^2} + \frac{\partial^2}{\partial z^2}.$$

The x-coordinate is measured vertically upward from the leading edge.

For $Gr \gg 1$, let us introduce the following scaled and non-dimensionalized variables for the flow in the corner layer (Region IV in Fig. 1):

$$(u, v, w) = \left[\frac{u^*}{U_c}, \frac{v^*}{U_c}\left(\frac{Gr}{4}\right)^{1/4}, \frac{w^*}{U_c}\left(\frac{Gr}{4}\right)^{1/4}\right]$$

$$p(\eta, \zeta) = \frac{p^*}{\rho U_c^2}\left(\frac{Gr}{4}\right)^{1/2}$$

$$\theta(\eta, \zeta) = (T - T_\infty)/(T_w - T_\infty) \tag{2}$$

$$\eta = \frac{y}{x}\left(\frac{Gr}{4}\right)^{1/4}, \quad \zeta = \frac{z}{x}\left(\frac{Gr}{4}\right)^{1/4}$$

where η and ζ are the stretched similarity variables and U_c denotes the convective velocity

$$U_c = \tfrac{1}{2}(g\beta\Delta Tx)^{1/2}.$$

Substitution of equations (2) into equations (1) yields the 'boundary-layer' equations appropriate to the problem (corner layer equation), when the most significant terms in each equation are retained

$$-\frac{1}{4}(\eta u_\eta + \zeta u_\zeta - 2u) + v_\eta + w_\zeta = 0 \tag{3a}$$

$$-\frac{u}{4}(\eta u_\eta + \zeta u_\zeta - 2u) + vu_\eta + wu_\zeta = \nabla^2 u + 4\theta \tag{3b}$$

$$-\frac{u}{4}(\eta v_\eta + \zeta v_\zeta + v) + vv_\eta + wv_\zeta = -p_\eta + \nabla^2 v \tag{3c}$$

$$-\frac{u}{4}(\eta w_\eta + \zeta w_\zeta + w) + vw_\eta + ww_\zeta = -p_\zeta + \nabla^2 w \tag{3d}$$

$$-\frac{u}{4}(\eta\theta_\eta + \zeta\theta_\zeta) + v\theta_\eta + w\theta_\zeta = \frac{1}{Pr}\nabla^2\theta \tag{3e}$$

where

$$\nabla^2 \equiv \frac{\partial^2}{\partial\eta^2} + \frac{\partial^2}{\partial\zeta^2}.$$

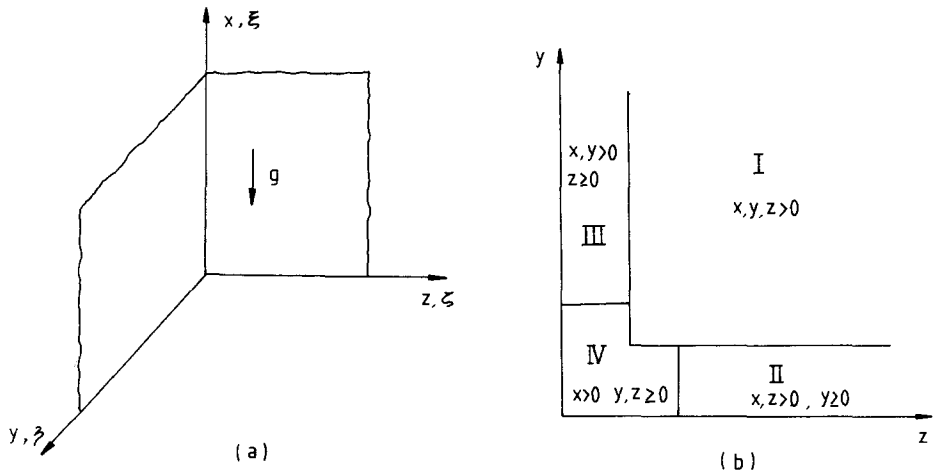

FIG. 1. Definition sketch: Region I, potential flow; Regions II and III, boundary layers; Region IV, corner layer.

The system of non-linear equations (3) is to be solved throughout the region $0 \leqslant \eta, \zeta \leqslant \infty$ subject to the appropriate boundary conditions.

2.2. *Boundary conditions*

In describing the boundary conditions for the corner layer equations, the following symmetry properties are to be noted:

$$\begin{aligned} u(\eta, \zeta) &= u(\zeta, \eta) \\ v(\eta, \zeta) &= w(\zeta, \eta) \\ \theta(\eta, \zeta) &= \theta(\zeta, \eta). \end{aligned} \tag{4}$$

2.2.1. *Wall boundary conditions.* The conditions on the wall are described simply by the no-slip and uniform wall temperature conditions

$$u = v = w = 0, \quad \theta = 1 \quad \text{at} \quad \eta = 0 \quad \text{and} \quad \zeta = 0. \tag{5}$$

2.2.2. *Far-field boundary conditions as* $\zeta \to \infty$, $\eta/\zeta \to 0$. The asymptotic boundary conditions for the corner layer are conveniently determined by requiring the consistent matching with the boundary layer from the corner. The conditions for u, v, and θ are obtained from the first-order boundary layer solutions as $z \to 0$. The condition for crossflow component w as $\zeta \to \infty$, however, can be posed only by considering the second-order boundary layer motion in Region II. The details of the derivation are fairly involved and only the main steps are given below, since the derivation can be carried out in parallel with Rubin [10].

With the known potential flow ($u = v = w = 0$, $\theta = 0$), the first-order boundary layer is introduced in order to satisfy the boundary condition $\theta = 1$ on the plates. As usual, the following scaled and dimensionless variables are introduced:

$$\begin{aligned} (\bar{u}, \bar{v}, \bar{w}) &= \left[\frac{u^*}{U_c}, \frac{v^*}{U_c}\left(\frac{Gr}{4}\right)^{1/4}, \frac{w^*}{U_c}\left(\frac{Gr}{4}\right)^{1/4}\right] \\ \bar{P} &= \frac{p^*}{\rho U_c^2}\left(\frac{Gr}{4}\right)^{1/2} \\ \bar{\theta} &= (T - T_\infty)/(T_w - T_\infty) \\ \bar{Y} &= \bar{y}\left(\frac{Gr}{4}\right)^{1/4}. \end{aligned} \tag{6}$$

Note that only the y-coordinate is stretched whereas the x- and z-coordinates are unchanged.

Substituting equations (6) into equations (1) and retaining the most significant terms in each equation, the well-known two-dimensional boundary layer equations are obtained

$$\begin{aligned} &\frac{\bar{u}}{2\bar{x}} + \frac{\partial \bar{u}}{\partial \bar{x}} + \frac{\partial \bar{v}}{\partial \bar{Y}} = 0 \\ &\frac{\bar{u}^2}{2\bar{x}} + \bar{u}\frac{\partial \bar{u}}{\partial \bar{x}} + \bar{v}\frac{\partial \bar{u}}{\partial \bar{Y}} = \bar{x}\frac{\partial^2 \bar{u}}{\partial \bar{Y}^2} + \frac{4\bar{\theta}}{\bar{x}} \\ &\bar{u}\frac{\partial \bar{\theta}}{\partial \bar{x}} + \bar{v}\frac{\partial \bar{\theta}}{\partial \bar{Y}} = \frac{1}{Pr}\bar{x}\frac{\partial^2 \bar{\theta}}{\partial \bar{Y}^2} \end{aligned} \tag{7}$$

$$\bar{u} = \bar{v} = 0, \quad \bar{\theta} = 1 \quad \text{at} \quad \bar{Y} = 0 \quad \text{and} \quad \bar{u} = \bar{\theta} \to 0 \quad \text{as} \quad \bar{Y} \to \infty.$$

The solution of equations (7) is given by

$$\begin{aligned} &\bar{u} = 4f'(\eta), \quad \bar{v} = \eta f'(\eta) - 3f(\eta) \\ &\bar{\theta} = t(\eta) \\ &\eta = \bar{Y}/\bar{x} = \frac{y}{x}\left(\frac{Gr}{4}\right)^{1/4} \end{aligned} \tag{8}$$

where $f(\eta)$ and $t(\eta)$ are the solutions of the natural

convection on a two-dimensional vertical flat plate

$$f'''(\eta)+3f(\eta)f''(\eta)-2[f'(\eta)]^2+t(\eta)=0$$
$$t''(\eta)+3Prf(\eta)t'(\eta)=0 \qquad (9)$$
$$f(0)=f'(0)=0, \quad t(0)=1, \quad f'(\infty)=t(\infty)=0.$$

The asymptotic matching condition implies that solution (8) provides the corner-layer behaviour of u, v, and θ as $\zeta\to\infty$. The remaining condition for w is determined by considering second-order boundary layer approximations. On emerging from the boundary layer, solution (8) exhibits a normal velocity

$$U_c\left(\frac{Gr}{4}\right)^{-1/4}\lim_{\eta\to\infty}\bar{v}(\eta)=\gamma U_c\left(\frac{Gr}{4}\right)^{-1/4} \quad \text{for } x>0$$

which is absent in zeroth-order potential flow. This velocity as well as the velocity on the opposite surface must serve as a matching condition for the next-order potential flow. Since the flow field outside the boundary layers must be irrotational, we write

$$(u^*,v^*,w^*)=(\Phi_x,\Phi_y,\Phi_z)$$
$$=U_c\left(\frac{Gr}{4}\right)^{-1/4}(U,V,W).$$

The function Φ is harmonic

$$\nabla^2\Phi=0 \qquad (10)$$

and the boundary conditions are, as a result of the matching conditions

$$\Phi_y=\gamma U_c\left(\frac{Gr}{4}\right)^{-1/4} \quad \text{at } y=0^+, x,z>0$$
$$=0 \qquad y=0^+, x\leqslant 0, z>0$$
$$\Phi_z=\gamma U_c\left(\frac{Gr}{4}\right)^{-1/4} \quad \text{at } z=0^+, x,y>0$$
$$=0 \qquad z=0^+, x\leqslant 0, y>0.$$

The solution of equation (10) for $x,y,z>0$ is given by

$$U(x,y,z)=\gamma\left[\bar{\zeta}^{-1}(1+\bar{\zeta}^2)^{-1/8}\left\{\left(\cos\frac{\theta_1}{4}-\sin\frac{\theta_1}{4}\right)-(1+\bar{\zeta}^2)^{1/2}\left(\cos\frac{3}{4}\theta_1+\sin\frac{3}{4}\theta_1\right)\right\}+\bar{\eta}^{-1}(1+\bar{\eta}^2)^{-1/8}\left\{\left(\cos\frac{\theta_2}{4}-\sin\frac{\theta_2}{4}\right)-(1+\bar{\eta}^2)^{1/2}\left(\cos\frac{3}{4}\theta_2+\sin\frac{3}{4}\theta_2\right)\right\}\right]$$
$$V(x,y,z)=\gamma(1+\bar{\eta}^2)^{-1/8}\left(\cos\frac{\theta_2}{4}-\sin\frac{\theta_2}{4}\right)$$
$$W(x,y,z)=\gamma(1+\bar{\zeta}^2)^{-1/8}\left(\cos\frac{\theta_1}{4}-\sin\frac{\theta_1}{4}\right) \qquad (11)$$

where

$$\bar{\eta}=y/x, \qquad \bar{\zeta}=z/x;$$
$$\theta_1=\tan^{-1}\bar{\zeta}, \quad \theta_2=\tan^{-1}\bar{\eta}.$$

The cross-flow component of velocity appears as a result of the mutual interaction of the boundary layers and this leads to a second-order boundary layer flow.

Since only the asymptotic condition for w in the corner layer is of interest, analysis of the secondary boundary layer will be limited to the cross-flow component of velocity. The second-order boundary layer equations for $\bar{u}$, $\bar{v}$, and $\bar{\theta}$ are in accord with that of the two-dimensional vertical flat plate [12]. The equation governing the $\bar{w}$-distribution is obtained from equation (1d), using the boundary layer variables (6)

$$-\frac{\bar{u}\bar{w}}{4\bar{x}}+\bar{u}\frac{\partial\bar{w}}{\partial\bar{x}}+\bar{v}\frac{\partial\bar{w}}{\partial\bar{Y}}=\bar{x}\frac{\partial^2\bar{w}}{\partial\bar{Y}^2},$$
$$\bar{w}=0 \text{ at } \bar{Y}=0, \ \bar{w}\to W(x,0,z) \text{ as } \bar{Y}\to\infty \qquad (12)$$

where W is given by equations (11).

For small $\bar{\eta}$ and $\bar{\zeta}$, the asymptotic behaviour of W is given by

$$W\sim\gamma\left(1-\frac{\bar{\zeta}}{4}-\frac{5}{32}\bar{\zeta}^2\right).$$

It may be assumed that, following Rubin [10]

$$\bar{w}\sim\gamma H_0'(\eta).$$

With $\bar{u}$ and $\bar{v}$ given by equations (8), the governing equation for $H_0'(\eta)$ becomes

$$H_0'''(\eta)+3f(\eta)H_0''(\eta)+f'(\eta)H_0'(\eta)=0$$
$$H_0'(0)=0, \quad H_0'(\infty)=1. \qquad (13)$$

The asymptotic boundary conditions as $\zeta\to\infty$ for the corner layer are described finally as follows:

$$u\sim 4f'(\eta), \quad v\sim\eta f'(\eta)-3f(\eta)$$
$$w\sim\gamma H_0'(\eta), \quad \theta\sim t(\eta). \qquad (14)$$

The conditions for the opposite plate can be obtained from symmetry conditions (4); as $\eta\to\infty$, $\zeta/\eta\to 0$

$$u\sim 4f'(\zeta), \qquad v\sim\gamma H_0'(\zeta)$$
$$w\sim\zeta f'(\zeta)-3f(\zeta), \quad \theta\sim t(\zeta). \qquad (15)$$

The corner layer problem is, thus, completely formulated by equations (3) and boundary conditions (5), (14), and (15).

The corner layer equations (3) are somewhat simplified by eliminating the pressure and introducing the 'velocity potentials'

$$\phi=\frac{\eta u}{4}-v, \quad \psi=\frac{\zeta u}{4}-w \qquad (16)$$

and the streamwise vorticity

$$\Omega=\psi_\eta-\phi_\zeta=\frac{\zeta}{4}u_\eta-\frac{\eta}{4}u_\zeta-(w_\eta-v_\zeta). \qquad (17)$$

The resulting equations are given by

$$\nabla^2 u + \phi u_\eta + \psi u_\zeta - \tfrac{1}{2}u^2 + 4\theta = 0$$

$$\nabla^2 \Omega + \phi \Omega_\eta + \psi \Omega_\zeta + u\Omega + \tfrac{3}{8}u(\eta u_\zeta - \zeta u_\eta) + \zeta\theta_\eta - \eta\theta_\zeta = 0$$

$$\nabla^2 \phi + \Omega_\zeta - u_\eta = 0$$

$$\nabla^2 \psi - \Omega_\eta - u_\zeta = 0$$

$$\frac{1}{Pr}\nabla^2\theta + \phi\theta_\eta + \psi\theta_\zeta = 0 \tag{18}$$

and the transformed boundary conditions are

$$u = \phi = \psi = 0, \quad \Omega = \psi_\eta, \quad \theta = 1 \quad \text{at } \eta = 0$$

$$u = \phi = \psi = 0, \quad \Omega = -\phi_\zeta, \quad \theta = 1 \quad \text{at } \zeta = 0$$

$$u \sim 4f'(\eta), \quad \phi \sim 3f(\eta), \quad \psi \sim \zeta f'(\eta) - \gamma H_0'(\eta)$$

$$\Omega \sim \zeta f''(\eta) - \gamma H_0''(\eta), \quad \theta \sim t(\eta) \quad \text{as } \zeta \to \infty$$

$$u \sim 4f'(\zeta), \quad \phi \sim \eta f'(\zeta) - \gamma H_0'(\zeta), \quad \psi \sim 3f(\zeta)$$

$$\Omega \sim -\eta f''(\zeta) + \gamma H_0''(\zeta), \quad \theta \sim t(\zeta) \quad \text{as } \eta \to \infty. \tag{19}$$

It is observed that the corner layer equations (18) and boundary conditions (19) are similar to those of Rubin [10, 11] except that the temperature equation is coupled with the flow field.

3. METHOD OF SOLUTION

Observation of the previous section shows that the computational domain is an infinite region and corner layer variables ϕ, ψ, and Ω become unbounded as η or $\zeta \to \infty$, which makes the numerical analysis of the problem somewhat inconvenient.

In order to avoid these inconveniences, we introduce new corner layer variables $\bar{\phi}$, $\bar{\psi}$, and $\bar{\Omega}$

$$\bar{\phi} = \phi - \eta f'(\zeta)$$

$$\bar{\psi} = \psi - \zeta f'(\eta) \tag{20}$$

$$\bar{\Omega} = \Omega + \eta f''(\zeta) - \zeta f''(\eta)$$

and transform the infinite region $0 \leqslant \eta, \zeta \leqslant \infty$ into a finite region $0 \leqslant N, S \leqslant 1$

$$N = \frac{a\eta}{1 + a\eta}, \quad S = \frac{a\zeta}{1 + a\zeta}. \tag{21}$$

With the above transformations, we can impose the asymptotic boundary conditions at true infinity and have the effect of increasing the resolution near the corner where large gradients are expected.

The final equations and boundary conditions are written in terms of new defined variables and solved numerically by the alternate direction implicit scheme. The mesh size and grid spacing parameter that should have a negligible effect on the solution were chosen through many numerical experiments

$$H = 0.02, \quad a = 0.2.$$

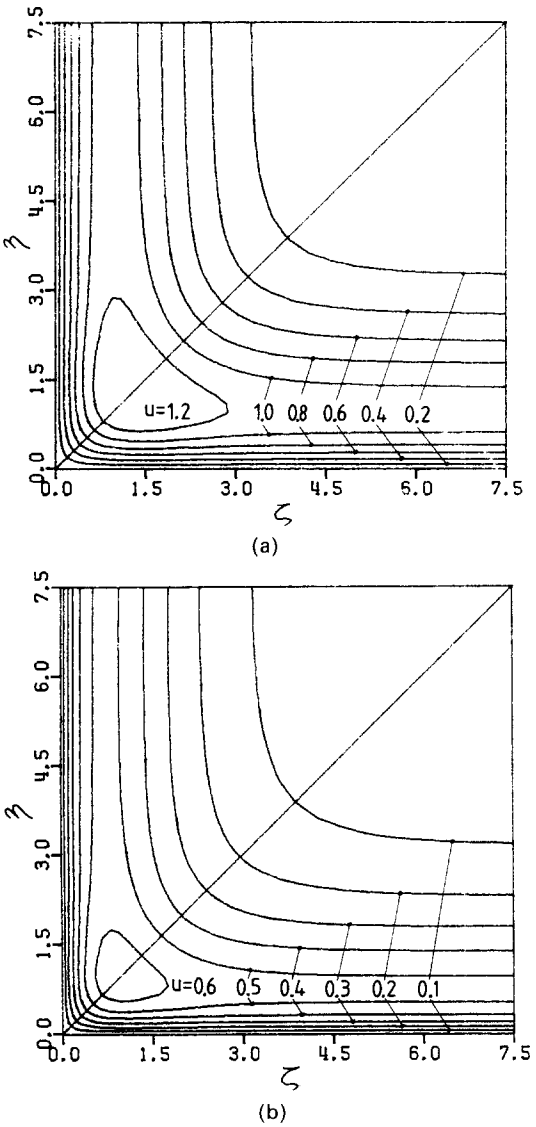

FIG. 2. Streamwise isovels: (a) $Pr = 0.72$; (b) $Pr = 7.0$.

Computations were made only for the variables u, $\bar{\Omega}$, $\bar{\phi}$, and θ in the region $0 \leqslant N, S \leqslant 1$ and $\bar{\psi}$ was determined from the symmetry property, $\bar{\psi}(N, S) = \bar{\phi}(S, N)$.

The solution is considered to be converged when the difference in the values of the dependent variables from successive iterations was less than 10^{-4} at every grid point.

4. RESULTS AND DISCUSSION

The numerical results for $Pr = 0.72$ and 7.0 are presented in Figs. 2–6. Figure 2 shows the isolines for streamwise velocity u. Observation of the velocity u shows that there is an inner region in which u is smaller than the asymptotic two-dimensional value. In this region, the effect of the coupling between the two plates leads to increasing the friction force and, therefore, decreasing the streamwise velocity, but outside

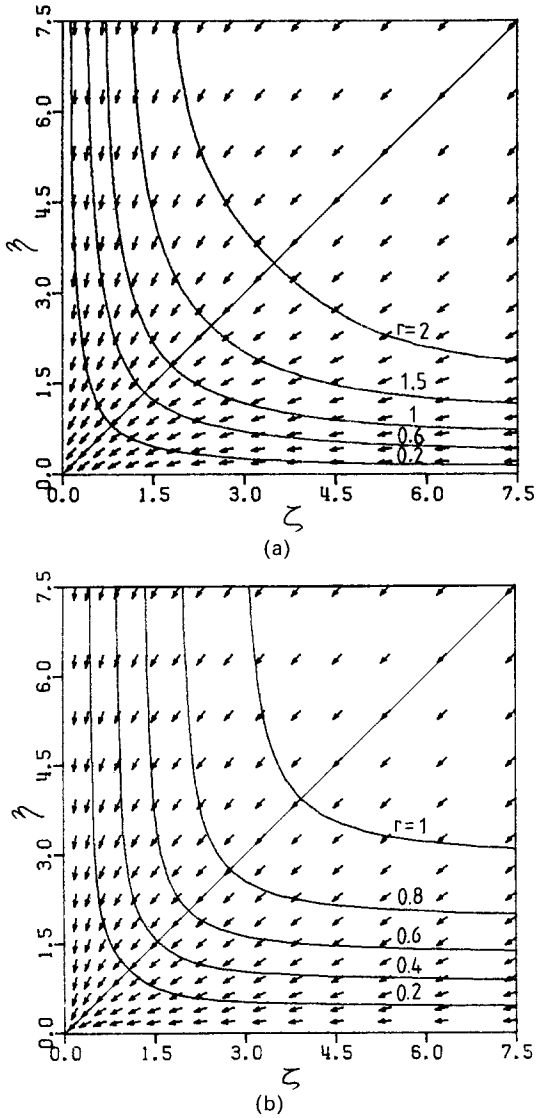

FIG. 3. Magnitudes and directions of crossflow: (a) $Pr = 0.72$; (b) $Pr = 7.0$.

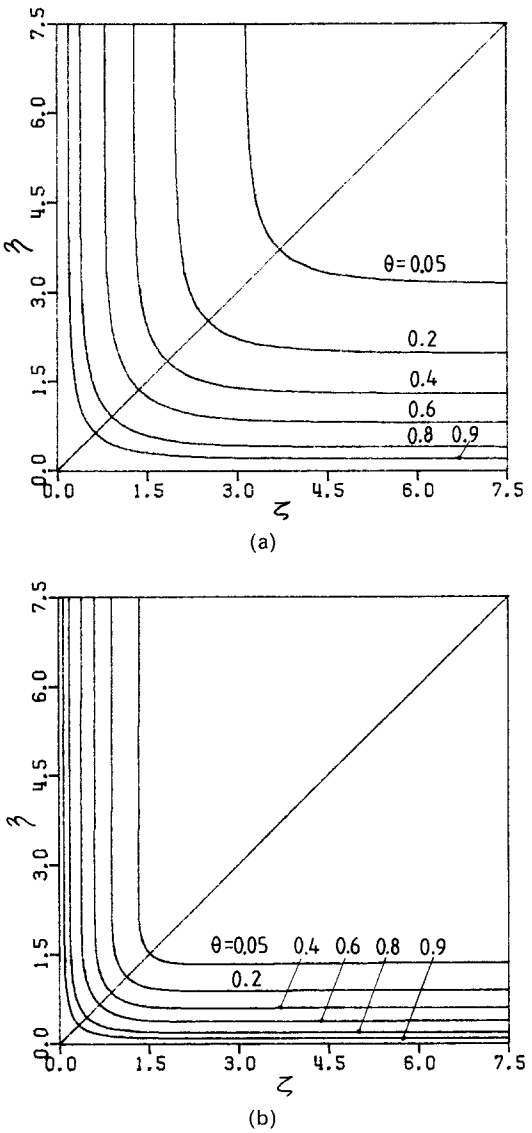

FIG. 4. Isotherms: (a) $Pr = 0.72$; (b) $Pr = 7.0$.

this region, the interaction of the boundary layer increases the buoyancy effect and accordingly the velocity u. The closed contour which is not present in the high-Reynolds number flow along a corner appears in the vicinity of the symmetry plane near the corner. This can be attributed to the increased amount of flow entrainment near the corner due to the mutual interaction of the two plates. The velocity boundary layer thickness has its maximum value at the symmetry plane and becomes thinner as ζ increases and ultimately approaches its asymptotic two-dimensional value.

In Fig. 3, isolines of $r = (v^2+w^2)^{1/2}$, the magnitude of the crossflow and the direction $\Theta = \tan^{-1}(v/w)$ are plotted. The magnitude of the crossflow, likewise the streamwise velocity, depends largely on Prandtl number and becomes greater as the distance from the corner increases. It is observed that the crossflow is directed almost radially inward to the corner, and does not show the swirling motion which is present in the high-Reynolds number flow. Considering the law of conservation of mass, this may also partly explain the presence of the closed contour of the streamwise isovels.

Figure 4 shows the temperature profiles for $Pr = 0.72$ and 7.0. The numerical results can be accurately (within 2% error) represented in terms of the solution of the natural convection on the two-dimensional vertical plate

$$1-\theta(\eta,\zeta) = [1-t(\eta)][1-t(\zeta)] \tag{22}$$

which is the solution of the following equation:

$$\frac{1}{Pr}\nabla^2\theta+3f(\eta)\theta_\eta+3f(\zeta)\theta_\zeta = 0. \tag{23}$$

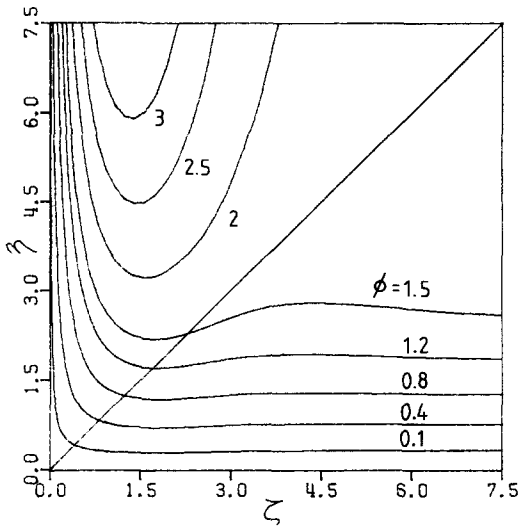

(a)

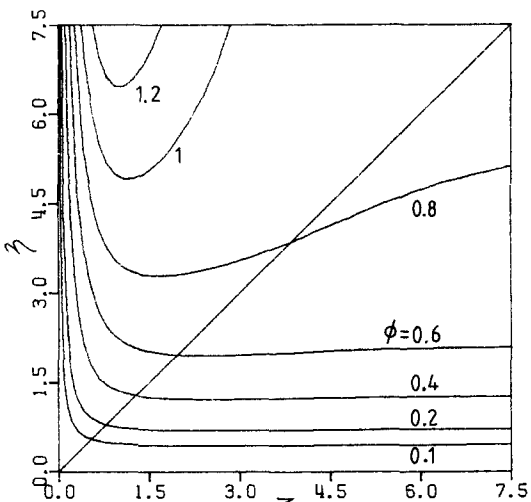

(b)

FIG. 5. Isolines of 'velocity potential', ϕ: (a) $Pr = 0.72$; (b) $Pr = 7.0$.

The approximate equation for θ, equation (23), can be obtained from the following observation. For large ζ and finite η, the term $\psi\theta_\zeta$ is much smaller than $\phi\theta_\eta$ since $\theta_\zeta \approx 0$ for large ζ. Also, as shown in Fig. 5, $\phi(\eta, \zeta)$ is nearly equal to $3f(\eta)$, the asymptotic two-dimensional value of ϕ, for $\zeta > \eta$. Near the corner, the conduction term in energy equation (18) is dominant. Taking into account the symmetry property and the above observations, we may approximate energy equation (18) to obtain equation (23).

Local heat transfer coefficients are available from the numerical solution. By definition

$$q = -k\frac{\partial T}{\partial y}\bigg|_{y=0} = h(T_w - T_\infty).$$

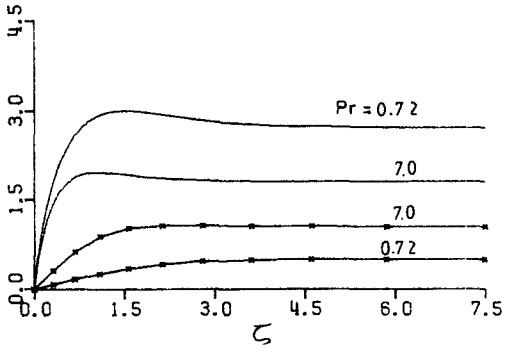

FIG. 6. Local Nusselt numbers and shear stresses: —*—*—, $Nu(0,\zeta)(Gr/4)^{-1/4}$; ——, $\tau_w(0,\zeta)(f''(0)/\tau_{w\infty})$.

The local Nusselt number is

$$Nu = \frac{hx}{k} = -\theta_\eta(0,\zeta)\left(\frac{Gr}{4}\right)^{1/4}. \tag{24}$$

In a similar fashion, the local shear stress on the plate results in, neglecting the effect of the secondary flow

$$\tau_w = \mu\frac{\partial u^*}{\partial y}\bigg|_{y=0} = u_\eta(0,\zeta)\frac{\tau_{w\infty}}{f''(0)} \tag{25}$$

where $\tau_{w\infty}$ is the asymptotic two-dimensional value

$$\tau_{w\infty} = \frac{\rho\nu^2}{x^2}f''(0)\left(\frac{Gr}{4}\right)^{3/4}.$$

Figure 6 shows Nu and τ_w for $Pr = 0.72$ and 7.0. The local Nusselt number Nu is zero at the corner line due to the symmetry of the temperature along the corner bisector, and increases monotonically to approach its asymptotic two-dimensional value. The local shear stress which is also zero at the corner line attains its maximum value at a certain distance from the vertex and then decreases to its asymptotic value corresponding to the two-dimensional natural convection problem. Considering the streamwise velocity profiles, it is found that the ζ-position of maximum shear stress is almost coincident with the position where the velocity u becomes largest. The variations of the local Nusselt number and shear stress with Prandtl number can be seen clearly in the figure.

REFERENCES

1. A. J. Ede, Advances in free convection. In *Advances in Heat Transfer*, Vol. 4, pp. 1–64. Academic Press, New York (1967).
2. H. K. Kuiken, Free convection at low Prandtl numbers, *J. Fluid Mech.* **37**, 785–798 (1969).
3. L. Pera and B. Gebhart, Natural convection boundary layer flow over horizontal and slightly inclined surfaces, *Int. J. Heat Mass Transfer* **16**, 1131–1146 (1973).
4. V. P. Carey, Analysis of transient natural convection flow at high Prandtl number using a matched asymptotic expansion technique, *Int. J. Heat Mass Transfer* **26**, 911–919 (1983).
5. T. S. Chen, H. C. Tien and B. F. Armaly, Natural con-

vection on horizontal, inclined, and vertical plates with variable surface temperature or heat flux, *Int. J. Heat Mass Transfer* **29,** 1465–1478 (1986).
6. J. H. Merkin and F. T. Smith, Free convection boundary layers near corners and sharp trailing edges, *ZAMP* **33,** 36–52 (1982).
7. R. Eichhorn and M. M. Hasan, Mixed convection about a vertical surface in cross-flow: a similarity solution, *ASME J. Heat Transfer* **102,** 775–777 (1980).
8. D. W. Hartfield and D. K. Edwards, Edge and aspect ratio effects on natural convection from the horizontal heated plate facing downwards, *Int. J. Heat Mass Transfer* **24,** 1019–1024 (1981).
9. C. Y. Liu and A. C. Guerra, Free convection in a porous medium near the corner of arbitrary angle formed by two vertical flat plates, *Int. Commun. Heat Mass Transfer* **12,** 431–440 (1985).
10. S. G. Rubin, Incompressible flow along a corner, *J. Fluid Mech.* **26,** 97–110 (1966).
11. A. Pal and S. G. Rubin, Asymptotic features of viscous flow along a corner, *Q. Appl. Math.* **29,** 91–108 (1971).
12. D. S. Riley and D. G. Drake, Higher approximations to the free convection flow from a heated vertical flat plate, *Appl. Scient. Res.* **30,** 193–207 (1975).

CONVECTION NATURELLE PRES D'UN COIN

Résumé—On considère le transfert thermique par convection naturelle laminaire au voisinage d'un coin formé par l'intersection de deux plans verticaux. Pour un grand nombre de Grashof les équations de couche limite sont dérivées et des conditions aux limites appropriées sont déterminées. Des solutions de ces équations sont obtenues numériquement pour les distributions de vitesse et de température, le nombre de Prandtl variant entre 0,72 et 7,0. Les configurations sont très différentes de celles relatives à l'écoulement pour des nombres de Reynolds élevés: on constate un écoulement simple d'entrée et le mouvement de tourbillonnement dans le coin n'existe pas.

NATÜRLICHE KONVEKTION IN EINER RECHTWINKLIGEN ECKE

Zusammenfassung—Es wird die laminare natürliche Konvektion in einer rechtwinkligen Ecke untersucht, die aus zwei vertikalen viertels-unendlichen ebenen Platten gebildet wird. Für große Grashof-Zahlen werden die Grenzschichtgleichungen für die Eckenströmung hergeleitet. Entsprechende Randbedingungen werden bestimmt unter Verwendung der Methode der angepaßten Reihenentwicklung. Es werden numerische Lösungen der Gleichungen für das Geschwindigkeits- und Temperaturfeld für die Prandtl-Zahlen 0,72 und 7,0 ermittelt. Das Kreuzströmungsverhalten ist ziemlich verschieden von der Strömung entlang der Ecke bei großen Reynolds-Zahlen. Das einfache Einströmungsverhalten in die Ecke erscheint. Die Wirbelströmung in der Ecke wurde nicht gefunden.

ЕСТЕСТВЕННАЯ КОНВЕКЦИЯ ВБЛИЗИ ДВУГРАННОГО УГЛА

Аннотация—Рассматривается теплоперенос при ламинарной естественной конвекции вблизи двугранного прямого угла, образованного пересечением двух вертикальных четверть-бесконечных плоских пластин. Для больших значений числа Грасгофа записаны уравнения пограничного слоя для жидкости вблизи угла и с использованием метода сращиваемых асимптотических разложений определены соответствующие граничные условия. Численным решением этих уравнений получены распределения скорости и температуры при числах Прандтля, равных 0,72 и 7,0. Течение в поперечном направлении имеет совершенно другой характер, нежели течение в продольном направлении. При большом значении числа Рейнольдса имеет место простое безвихревое течение по направлению к ребру угла.